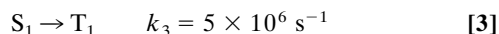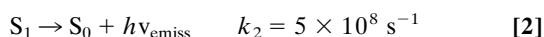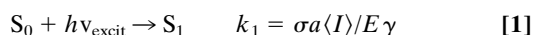# Supporting Information

Vukojević *et al.* 10.1073/pnas.0809250105

SI Text

Numerical Simulation of Singlet–Triplet Transition Kinetics. To verify that fluorescence intensity is gained by abolishing intersystem crossing, we emulated numerically the kinetics of basic electron transition pathways in fluorescence (Fig. S1 *C*). Numerical simulations (Fig. S1*D*) show that maximum occupancy of the triplet state (T_1) is reached markedly slower than the maximum occupancy of the first excited singlet state (S_1). Thus, whereas S_1 becomes fully populated nearly instantaneously after photon absorption, T_1 remains unsaturated for longer times and there is a time window, $\theta < 1\ \mu$s, where the relative occupancy of S_1 compared with T_1 is favorable for fluorescence emission. Kinetics of the physical processes underlying fluorescence becomes relevant at short observation times and caused the experimentally observed gain in fluorescence intensity.

Numerical simulations. We analyzed the simplified energy diagram showing processes that accompany fluorophore excitation by photon absorption to the first excited electronic level (S_1), its subsequent relaxation to the ground energy level (S_0) by fluorescence emission and fluorescence loss due to intersystem crossing to the triplet state (T_1) (Fig. S1 *C*). For numerical simulations, the following "reaction" scheme is built:

$$S_0 + h\nu_{\text{excit}} \rightarrow S_1 \qquad k_1 = \sigma a \langle I \rangle / E\gamma \qquad [1]$$

$$S_1 \rightarrow S_0 + h\nu_{\text{emiss}} \qquad k_2 = 5 \times 10^8\ \text{s}^{-1} \qquad [2]$$

$$S_1 \rightarrow T_1 \qquad k_3 = 5 \times 10^6\ \text{s}^{-1} \qquad [3]$$

Rate equations were derived in accordance to the mass-action law. For continuous-wave irradiation, the excitation rate is proportional to the absorption cross-section of the fluorophore (σ_a), the continuous-wave irradiance $\langle I \rangle$ and reciprocal to the laser photon energy (E_γ). To simulate the fluorescence excitation/emission for different irradiance, the following values of k_1 were selected for numerical simulations: low irradiance, $k_1 = 1 \times 10^4\ \text{s}^{-1}$; moderate irradiance, $k_1 = 8 \times 10^7\ \text{s}^{-1}$; high irradiance, $k_1 = 1 \times 10^9\ \text{s}^{-1}$. The initial concentration of the fluorophore in the ground state was $[S_0]_0 = 10$ nM. Numerical simulations were carried out by using the Gepasi 3.30 software package for modeling biochemical systems (1) and a software for numerical integration of kinetic equations with a fifth-order Runge Kutta method (2).

Determination of Molecular Numbers by Quantitative CLSM. Molecular numbers determined by quantitative CLSM imaging compared with values obtained by FCS are given in Table S1.

Imaging Mobile Molecules by Quantitative CLSM. In Fig. S2, images of live neuroblastoma cells expressing the Enhanced Green Fluorescent Protein (EGFP) were acquired by slow (Fig. S2*B*) and fast (Fig. S2*C*) scanning. In the slowly acquired image the scanning time, $\tau_{\text{Scan}} = 328\ \mu$s, is longer than the diffusion time of EGFP, $\tau_{\text{Diff}} = 140\ \mu$s. Hence, EGFP motion is captured by imaging, and short stretches of illuminated pixels indicating EGFP movement in the scanning direction are visible in the image. In the image acquired by fast scanning (Fig. S2*C*) the scanning time, $\tau_{\text{Scan}} = 19.4\ \mu$s, is considerably shorter than the diffusion time of EGFP, and EGFP molecules appear to be "frozen" in the pixel box. Examples of diffusion rates typically encountered in live cells and scanning speeds recommended for CLSM imaging are given in Table S2.

1. Mendes P (1997) Biochemistry by numbers: Simulation of biochemical pathways with Gepasi 3. *Trends Biochem Sci* 22:361–363.

2. Vukojević V, Sørensen PG, Hynne F (1996) Predictive value of a model of the Briggs-Rauscher reaction fitted to quenching experiments. *J Phys Chem* 100:17175–17185.
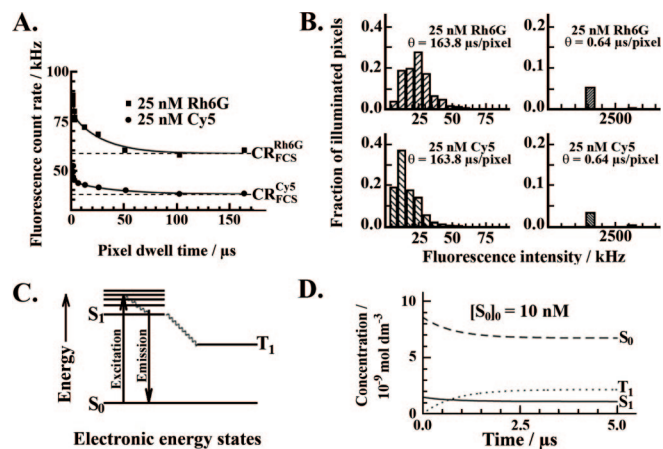
Fig. S1. Fluorescence intensity gain by fast scanning due to abolished intersystem crossing. (*A*) Dependence of the average fluorescence count rate ($CR_{\mathrm{image}}^{\theta}$) on the scanning speed. The corresponding value measured by FCS (CR_{FCS}) is given by the dashed lines. (*B*) Fluorescence intensity distribution in images acquired by slow (sparsely striped bars) and fast scanning (densely striped bars). (*C*) Simplified electronic energy diagram for a typical organic fluorophore indicating major electron transition pathways in fluorescence excitation/loss. Fluorescence is excited through photon absorption followed by a nearly instantaneous redistribution of electrons in the fluorophore from the ground electronic state (S_0) to the vibrationally excited upper electronic state (S_1). Nonradiative transition from the excited singlet state to the metastable triplet state, $S_1 \rightarrow T_1$, is known as intersystem crossing. Although it is a significantly slower process, intersystem crossing is concurrent to fluorescence emission, $S_1 \rightarrow S_0$, because of its comparatively long lifetime. In addition, enhanced reactivity of the triplet state compared with the singlet state may lead to irreversible fluorescence loss. (*D*) Numerical integration of the kinetics of fluorescence excitation/emission showing that during short observation times, $\theta < 1\ \mu s$, the triplet state T_1 is not saturated and relative occupancy of the S_1 versus T_1 states is favorable for fluorescence emission. The initial concentration of the fluorophore in the ground state was $[S_0]_0 = 10$ nM.
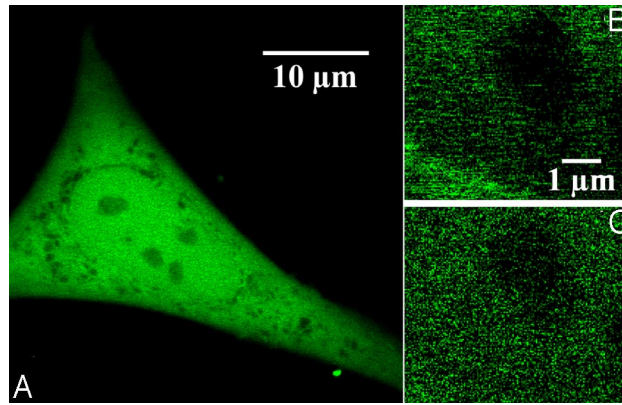
Fig. S2. Imaging molecular diffusion in live cells. (*A*) Confocal APD image of a neuroblastoma cell expressing EGFP acquired by slow scanning, $\theta = 51.2$ μs per pixel, and without averaging. (*B*) Magnified detail of *A*, showing the border between the nucleus and the perinuclear region. Stretches of illuminated pixels indicate EGFP movement in the scanning direction that was captured by imaging. (*C*) In the image acquired by fast scanning, $\theta = 3.2$ μs per pixel, molecular movement is no longer observable.

Table S1. Average number of fluorescent molecules in the observation volume element determined by CLSM imaging compared with the average number of molecules in the observation volume element determined by FCS

Sample	Image analysis			$\bar{N}_{FCS}$
	$\bar{i}_p$	σ^2	$\bar{N}_{image}$	
40 nM Rh6G	3.9	4.0	3.8	4.0
10 nM Rh6G	1.1	1.0	1.2	1.2
20 nM Cy5	2.4	2.6	2.2	2.3
10 nM Rh6G + 20 nM Cy5-dsDNA-Rh6G green	3.7	3.6	3.7	3.5
red	2.3	2.3	2.3	2.7
20 nM quantum dots	1.0	1.0	1.0	1.2

Table S2. Scanning speeds recommended for quantitative imaging of moving molecules

Pixel dwell time (θ), μs/pixel	Scanning time (τ_{Scan}),* μs	Diffusion constant (D), m^2 s^{-1}	Diffusion time (τ_{Diff}), μs	Object
0.64–1.27	3–8	3×10^{-10}	35	Organic dye, small molecules
3.2–6.4	15–40	5×10^{-11}	200	Proteins in solution
64–100	350–600	3×10^{-12}	3,500	Cell surface receptor

The diffusion coefficients given as examples correspond to values typically encountered in live cells.

*Relation between the pixel dwell time and the scanning time is given by Eq. **14**. In our experiments $\tau_{Scan} = 6 \cdot \theta$.